Vaccine 37 (2019) 1266–1276

Contents lists available at ScienceDirect

Vaccine

journal homepage: www.elsevier.com/locate/vaccine

Viral vector and route of administration determine the ILC and DC profiles responsible for downstream vaccine-specific immune outcomes

S. Roy [a,1], M.I. Jaeson [a,1], Z. Li [a], S. Mahboob [a], R.J. Jackson [a], B. Grubor-Bauk [b], D.K. Wijesundara [a,b], E.J. Gowans [b], C. Ranasinghe [a,*]

[a] Molecular Mucosal Vaccine Immunology Group, Department of Immunology and infectious Disease, The John Curtin School of Medical Research, The Australian National University, Canberra ACT 2601, Australia
[b] Virology Group, Basil Hetzel Institute for Translational Health Research, University of Adelaide, Australia

ARTICLE INFO

Article history:
Received 9 July 2018
Received in revised form 8 January 2019
Accepted 23 January 2019
Available online 4 February 2019

Keywords:
ILC
DC
Viral vector-based vaccines
IL-13
IFN-γ
IL-17
Mucosal and systemic vaccination

ABSTRACT

This study demonstrates that route and viral vector can significantly influence the innate lymphoid cells (ILC) and dendritic cells (DC) recruited to the vaccination site, 24 h post delivery. Intranasal (i.n.) vaccination induced ST2/IL-33R$^+$ ILC2, whilst intramuscular (i.m.) induced IL-25R$^+$ and TSLPR$^+$ (Thymic stromal lymphopoietin protein receptor) ILC2 subsets. However, in muscle a novel ILC subset devoid of the known ILC2 markers (IL-25R$^-$ IL-33R$^-$ TSLPR$^-$) were found to express IL-13, unlike in lung. Different viral vectors also influenced the ILC-derived cytokines and the DC profiles at the respective vaccination sites. Both i.n. and i.m. recombinant fowlpox virus (rFPV) priming, which has been associated with induction of high avidity T cells and effective antibody differentiation exhibited low ILC2-derived IL-13, high NKp46$^+$ ILC1/ILC3 derived IFN-γ and low IL-17A, together with enhanced CD11b$^+$ CD103$^-$ conventional DCs (cDC). In contrast, recombinant Modified Vaccinia Ankara (rMVA) and Influenza A vector priming, which has been linked to low avidity T cells, induced opposing ILC derived-cytokine profiles and enhanced cross-presenting DCs. These observations suggested that the former ILC/DC profiles could be a predictor of a balanced cellular and humoral immune outcome. In addition, following i.n. delivery Rhinovirus (RV) and Adenovius type 5 (Ad5) vectors that induced elevated ILC2-derived IL-13, NKp46$^+$ ILC1/ILC3-derived-IFN-γ and no IL-17A, predominantly recruited CD11b$^-$ B220$^+$ plasmacytoid DCs (pDC). Knowing that pDC are involved in antibody differentiation, we postulate that i.n. priming with these vectors may favour induction of effective humoral immunity. Our data also revealed that vector-specific replication status and/or presence or absence of immune evasive genes can significantly alter the ILC and DC activity. Collectively, our findings suggest that understanding the route- and vector-specific ILC and DC profiles at the vaccination site may help tailor/design more efficacious viral vector-based vaccines, according to the pathogen of interest.

1. Introduction

In the last two decades, inactivated, live attenuated, replication-competent or -defective viruses have been extensively tested as viral vector-based vaccines. Interestingly, poxviruses such as Modified Vaccinia Ankara (MVA), New York strain of vaccinia virus (NYVAC), which are attenuated versions of vaccinia virus (VV), and Avipoxvirus; canarypox and fowlpox (FPV) viruses, used in prime-boost modalities have yielded uniquely different immune outcomes, dependent upon the route of delivery and/or the vaccine vector combination [1–4]. For example, heterologous rFPV/rVV compared to rVV/rFPV vaccination has shown to induce highly poly-functional/ high avidity T cells [3,5–7], moreover, rMVA used as a booster, as opposed to a prime has shown to induce more effective T cell immunity [8–10]. Similarly, both replication-competent and -defective recombinant Adenovirus-based vaccines have also shown to induce T cell responses associated with immune protection in animal models [11–13]. Moreover, viruses such as, Influenza A, Human RV, Cytomegalovirus, and Vesicular stomatitis virus, have also been assessed as promising vaccine delivery vehicles [10,14–16]. In a recent prime-boost vaccination study, mucosal RV prime vaccination was shown to induce HIV-specific T cell responses associated with protection in mice [17]. To improve vaccine-specific immunity, variants of viral vectors,

* Corresponding author.
E-mail address: Charani.Ranasinge@anu.edu.au (C. Ranasinghe).
[1] Authors contributed equally to the work.

https://doi.org/10.1016/j.vaccine.2019.01.045
0264-410X/

such as IL-1βR and/or IL18 binding protein (IL-18bp) deletion mutants of MVA and Adenoviral vectors have also been recently tested [18–20]. Despite the knowledge of different viral vector-based vaccines conferring different adaptive immune outcomes, the underlying innate immune mechanisms governing these processes at the vaccination site still remains elusive, specifically the role of innate lymphoid cells (ILCs) and dendritic cells (DCs).

ILCs, although derived from a common progenitor, are lineage negative in nature and according to the transcription factors, receptors and cytokines they express, are broadly classified into three main categories (ILC1, ILC2 and ILC3) [21]. ILC2, due to their ability to express IL-13, have been heavily studied under chronic inflammation, allergic asthma and helminth infections [22]. During intracellular pathogen infection, ILC1 have shown to express IFN-γ and tumour necrosis factor (TNF)-α [23], whilst during extracellular bacterial and fungal infections, ILC3 have been associated with interleukin (IL)-17A and IL-22 expression [24,25]. Although ILCs have three distinct phenotypes, studies have shown that they have the ability to interconvert between the phenotypes, according to the external stimuli, and thus thought to be highly plastic [26,27]. It is postulated that ILCs can polarize the immune response, according to the immune cell milieu or pathogen encountered, towards Th1, Th2 or Th17 immunity. However, the role of ILCs in viral vector-based vaccination is not well characterised.

DCs sample antigens at various body surfaces; skin, gastrointestinal tract and lungs, and are among the first line of defence against many pathogens. Based on the anatomical location and the invading pathogen, distinct DC subsets carry out differential functions [28]. For example; lung DCs have been extensively studied under respiratory infections. Lung conventional $CD11b^+$ $CD103^-$ DCs (cDCs) and cross-presenting $CD11b^-$ $CD103^+$ DCs have been associated with CD8 T cell priming [29,30]. Although conflicting evidence suggest that cDCs are functionally more important in mounting an effective antiviral response [31,32], there is growing evidence to support the notion that the activity of a particular DC subset is determined by the specific infection. For example: control of acute influenza virus infection is associated with $CD11b^-$ $CD103^+$ DCs cross presentation to CD8 T cells [33], whilst, $CD11b^-$ $CD8^+$ DCs, which share a common developmental origin with $CD11b^-$ $CD103^+$ DCs, have been associated with activation of cytotoxic CD8 T cells against non-respiratory pathogens such as West Nile Virus [34]. In the context of respiratory syncytial virus (RSV) infection, $CD11b^+$ and $CD103^+$ DC subsets have been involved in antigen presentation to both CD4 and CD8 T cells [35]. In addition, during Influenza A infection, $CD11b^+$ DCs have also been associated with humoral immunity [36]. Furthermore, plasmacytoid DCs (pDCs) also have been associated with distinct functions during viral infections [37,38].

It is now well established that the route of delivery, cytokine milieu, viral vectors and the order in which they are administered can yield vastly different adaptive immune outcomes [3,5,7,39,40]. We have previously shown that (i) IL-13, although detrimental for high avidity/poly-functional CD8 T cell immunity, was necessary for effective antibody differentiation [41–43]. (ii) Using rFPV adjuvanted vaccines that transiently inhibited IL-13 activity at the vaccination site, we have recently established that ILC2 (not other $lineage^+$ cells) were the major source of IL-13 at the vaccination site 24 h post vaccination [44]. (iii) Furthermore, using the same vaccines we have also shown that elevated IL-13 in the milieu recruited $CD11b^-$ $CD103^+$ cross-presenting DCs, associated with low avidity CD8 T cells [42,45]. Therefore, in this study to further understand which specific innate immune cell subsets play a predominant role in shaping the downstream adaptive immune outcomes, replicating and non-replicating viral vectors were delivered intranasally and intramuscularly and subsequent ILC-derived cytokine profiles and DCs subsets were assessed 24 h post vaccination.

2. Results

2.1. Different viral vector-based vaccines can induce uniquely different ILC2-derived 13 profiles following intranasal and intramuscular vaccination

BALB/c mice were vaccinated intranasally or intramuscularly with four different poxviral vectors rFPV, rMVA, rVV and rMVAΔIL-1βR and three non-poxviral vectors Influenza A, Human rhinovirus (RV) and Adenovirus type 5 (Ad5). Percentage of lung and muscle ILC2 and their corresponding IL-13 expression were assessed 24 h post vaccination. ILC2 were gated as $CD45^+$ FSC^{low}, SSC^{low}, $lineage^-$ $ST2/IL\text{-}33R^+$ cells for lung (**Fig. S1**) or $lineage^-$ $IL\text{-}25R^+$, $TSLPR^+$ and $ST2/IL\text{-}33R^+$ for muscle (**Fig. S2**), as indicated in Materials and Methods and Li et al 2018 [44]. Among all the vectors tested, following i.n. delivery, Influenza A vector recruited the highest percentage of Lin^- $ST2/IL\text{-}33R^+$ ILC2 to the vaccination site (lung mucosae). In contrast, RV and Ad5 recruited the lowest percentage of ILC2, which was much lower than unimmunized control ($p = 0.0014$ *and* $p = 0.0011$ respectively) (Fig. 1**A and S3**). However, despite this, RV and Ad5 expressed elevated IL-13 levels, which were similar to rMVA and Influenza A (Fig. 1**B**). Among the three poxviral vectors tested, the highest IL-13 level was detected in rMVA (rFPV vs rMVA $p < 0.0001$, rMVAΔIL-1βR vs rMVA $p < 0.0001$), whilst rMVAΔIL-1βR showed the lowest (rFPV vs rMVAΔIL-1βR $p = 0.4159$) (Fig. 1**B**). It is also noteworthy that, all the vectors showed significantly elevated IL-13 expression by Lin^- $ST2/IL\text{-}33R^+$ ILC2 compared to the unimmunized control (rFPV $p = 0.0028$; rMVA $p < 0.0001$; rMVAΔIL-1βR $p = 0.0412$; Influenza A $p < 0.0001$; RV $p < 0.0001$; Ad5 $p < 0.0001$) (Fig. 1**A and B**).

Following i.m. vaccination, mainly $IL\text{-}25R^+$ ILC2s and $TSLPR^+$ ILC2, ranging from 0.25% to 2% were detected. In the context of $IL\text{-}25R^+$ ILC2, rMVA and Ad5 vector vaccination showed significantly elevated numbers compared to unimmunised control ($p = 0.0183$ *and* $p = 0.0178$ respectively). Furthermore, Ad5 vaccination also showed higher proportion of $IL\text{-}25R^+$ ILC2s compared to influenza A ($p = 0.0004$) (Fig. 1**G, H and I**). Interestingly, rMVAΔIL-1βR (1.8% average) showed a significantly elevated proportion of $TSLPR^+$ ILC2 compared to rFPV and rMVA vaccination ($p < 0.0001$ and $p = 0.0240$ *respectively*) (Fig. 1**G, H and I**). Ad5 also showed elevated $TSLPR^+$ ILC2s compared to rFPV and influenza A vaccination ($p = 0.0103$ and $p = 0.0006$ respectively) (Fig. 1**G, H and I**). Following i.m. vaccination, similar to our previous studies extremely low or no $ST2/IL\text{-}33R^+$ ILC2 were detected with all vaccine groups tested (Fig. 1**G, H and I**).

Surprisingly, following i.m. delivery, canonical ILC2 subsets ($IL\text{-}25R^+$, $TSLPR^+$) were found to express marginal IL-13. In contrast, compared to the unimmunised control, a not yet defined ILC2 subset that lacked IL-25R, ST2/IL-33R and TSLPR were found to express IL-13 (Fig. 1**E and F**). Out of the vectors tested, Ad5 showed remarkably higher proportion (2 to 3-fold) of $IL\text{-}25R^-$ $IL\text{-}33R^-$ $TSLPR^-$ cells expressing IL-13 ($p < 0.0001$) (Fig. 1**E and F**), which was comparatively lower than i.n. Ad5 vaccination (Fig. 1**B**). It is noteworthy that, the ILC2-derived IL-13 expression by each vector was significantly higher following i.m. delivery compared to i.n. delivery. (Note that: The parent ILC2 population in the i.m. groups were much greater than the i.n. $ST2^+/IL\text{-}33R^+$ ILC2s. Thus, the difference in IL-13 expression by these two ILC subsets were also represented normalised to the $CD45^+$ subset, described in materials and methods (Fig. 1**J**).

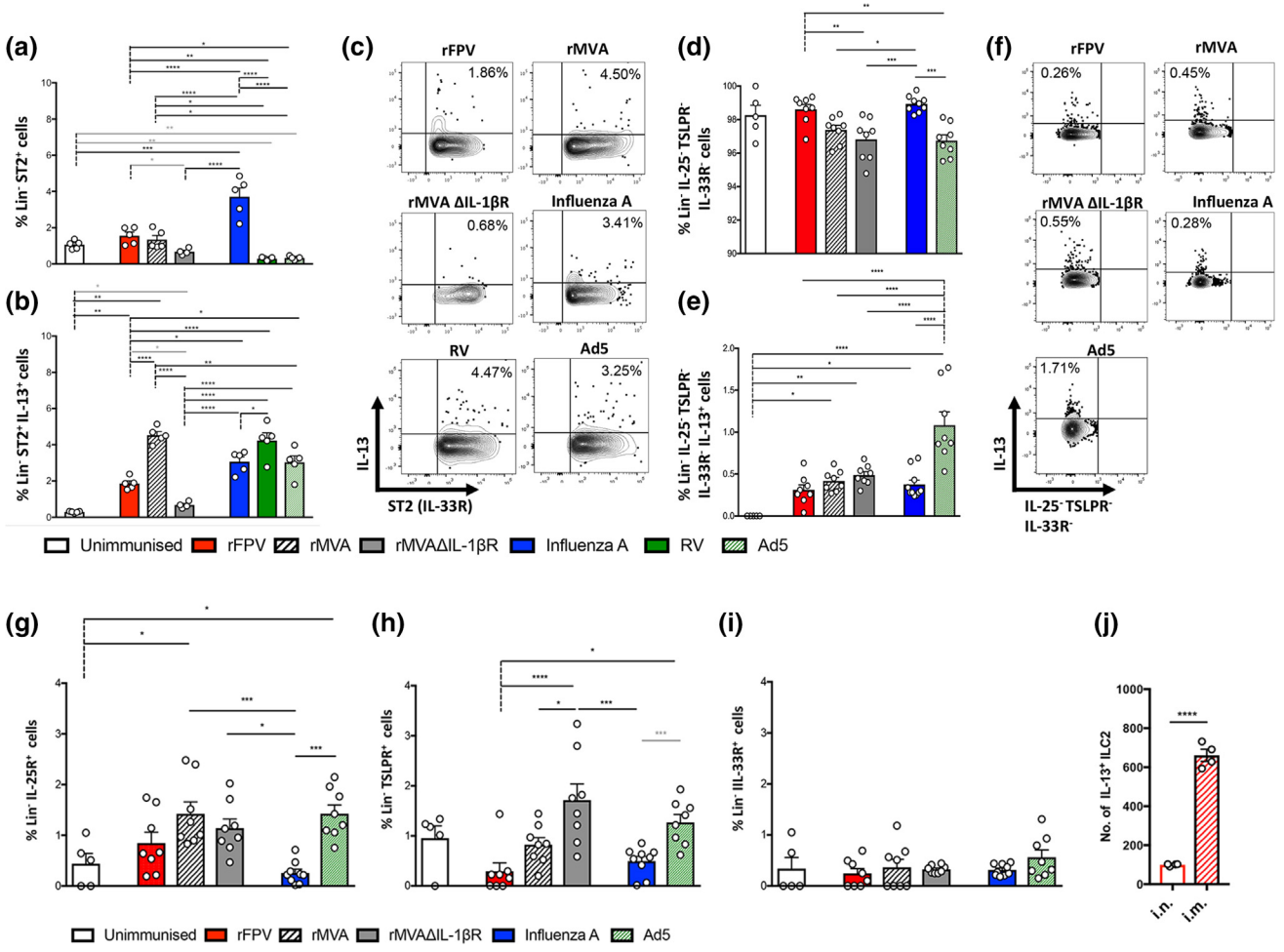

Fig. 1. Evaluation of lung and muscle ILC2 and corresponding IL-13 expression following intranasal and intramuscular viral vaccination. BALB/c mice (n = 5–9 per group) were i.n. or i.m. immunised with rFPV, rMVA, rMVA-ΔIL-1βR, Influenza A, RV or Ad5. 24 h post vaccination lungs were harvested and single cell suspensions were stained for ILC2s and their IL-13 expression and analysed using flow cytometry. Cells were pre-gated on $CD45^+$ FSC^{low} SSC^{low} cells using FlowJo software as described in Materials and Methods and **Figs. S1 and S2**. Lung ILC2 graphs show **(A)** the percentage of Lin^- ST2/IL-33R$^+$ ILC2 and **(B)** IL-13 expression by Lin^- ST2/IL-33R$^+$ ILC2. **(C)** Representative FACS plots show percentage of Lin^- ST2/IL-33R$^+$ ILC2 expressing IL-13. Muscle ILC2 graphs show percentage of **(D)** Lin^- IL-25R$^-$ TSLPR$^-$ ST2/IL-33R$^-$ ILC2 and **(E)** IL-13 expression by this novel ILC2 subset. **(F)** Representative FACS plots show percentage of Lin^- IL-25R$^-$ TSLPR$^-$ ST2$^-$/IL-33R$^-$ ILC2 expressing IL-13, and graphs show muscle **(G)** IL-25R$^+$ ILC2s, **(H)** TSLPR$^+$ ILC2s and **(I)** ST2$^+$/IL-33R$^+$ ILC2s. To compare and contrast lung and muscle ILC2-derived IL-13, **(J)** bar graph represents IL-13 expression by Lin^- ST2/IL-33R$^+$ ILC2 (i.n.) and Lin^- IL-25$^-$ TSLPR$^-$ ST2/IL-33R$^-$ ILC2 (i.m.) following rFPV vaccination. Error bars represent Standard Error of mean (SEM) and p values were calculated using One-way ANOVA followed by Tukey's multiple comparison test (black lines) and paired student's *t* test (grey lines). $^*p < 0.05$, $^{**}p < 0.01$, $^{***}p < 0.001$, $^{****}p < 0.0001$. Experiments with each vector were repeated minimum 2–3 times.

2.2. Poxviral and non-poxviral vectors showed significantly different ILC1/ILC3- derived IFN-γ and IL-17A expression profiles

Our recent intranasal rFPV vaccination studies have shown that the transient inhibition of ILC2-derived IL-13 at the vaccination site can directly impact the level of IFN-γ and IL-17A expression by NKp46$^+$ and NKp46$^-$ ILC1/ILC3s at the vaccination site 24 h post vaccination [44]. Hence, we next investigated the induction of IFN-γ and IL-17A expression by ILC1/ILC3s by different viral vaccine vectors as per indicated in Materials and Methods using flow cytometry gating strategies described in **Fig. S1.** Following i.n. vaccination, although no significant differences in the percentages of NKp46$^+$ ILC1/ILC3s were detected compared to the unimmunized control (Fig. 2**A**), compared to Influenza A, Ad5 showed significantly reduced numbers of NKp46$^+$ ILC1/ILC3s ($p = 0.042$). Whist rMVAΔIL-1βR recruited NKp46$^+$ ILC1/ILC3s similar to rFPV, rMVA recruited significantly lower numbers of NKp46$^+$ ILC1/ILC3s compared to rFPV ($p = 0.036$). In the context of IFN-γ expression by NKp46$^+$ ILC1/ILC3s, RV induced the highest (average 14.5%), followed by Ad5 (average 5%) and rFPV (average 2.9%) (Fig. 2**B**). Unlike rFPV, the deletion mutant rMVAΔIL-1βR and rMVA showed significantly lower IFN-γ expression ($p = 0.0187$, and 0.0011 respectively), which was also lower than the unimmunized control ($p = 0.0086$ respectively) (Fig. 2**B**). Expression of IFN-γ by Influenza A was similar to that of the unimmunized control.

Interestingly, following i.n. delivery 95–98% ILC1/ILC3s were found to be NKp46$^-$ (Fig. 2**A and D).** Although there were no differences observed between the numbers of NKp46$^-$ ILC1/ILC3s recruited by any of poxvirus vectors (Fig. 2**D**), IFN-γ expression was vastly different. rFPV was amongst the highest inducers of IFN-γ expression by NKp46$^-$ ILCs (Fig. 2**E**), whilst showing modest IFN-γ expression also by NKp46$^+$ ILCs (Fig. 2**B**). Out of all the vaccine vectors tested, rMVAΔIL-1βR showed the lowest IFN-γ expression by NKp46$^-$ ILC1/ILC3s (Fig. 2**E**). Although Influenza A recruited significantly lower numbers of NKp46$^-$ ILC1/ILC3s compared to RV and Ad5 ($p = 0.0004$, $p < 0.0001$ respectively), it induced the highest IFN-γ expression among the non-poxviral vectors (Fig. 2**E).** Interestingly, the IFN-γ expression by NKp46$^-$ ILC1/ILC3s was very similar between Influenza A and rFPV vaccinated groups (Fig. 2**E**). It is noteworthy that, although the unimmunized

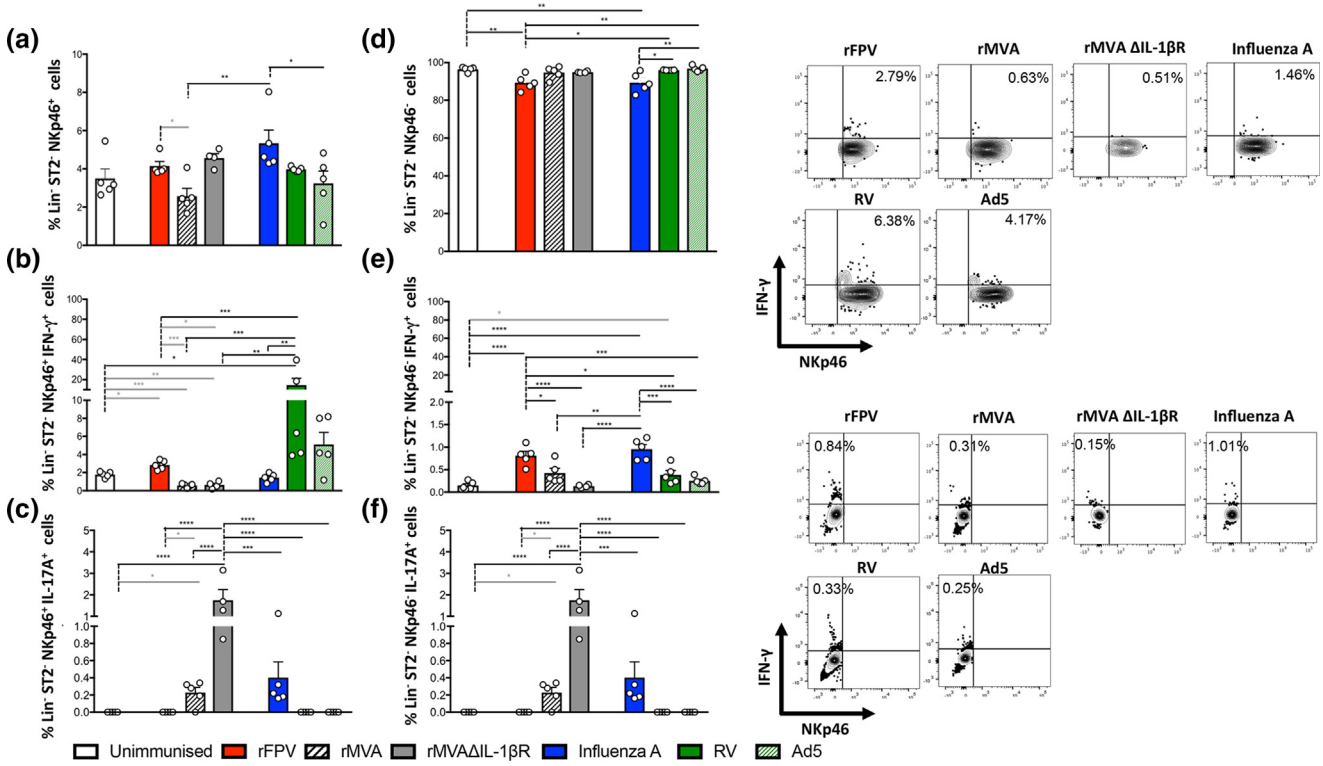

Fig. 2. Evaluation of lung Lin⁻ ST2⁻ NKp46⁺ and NKp46⁻ ILC-derived IFN-γ and IL-17A expression following intranasal viral vector vaccination. BALB/c mice (n = 5) were i.n. immunised with same vectors as per in Fig. 1, and stained for Lin⁻ ST2/IL-33R⁻ NKp46⁺ and NKp46⁻ ILC and their cytokine expression. Cells were pre-gated on CD45⁺ FSC^{low} SSC^{low} cells as described in Materials and Methods and **Fig. S1**. Graphs show percentage of **(A)** Lin⁻ ST2/IL-33R⁻ NKp46⁺ ILC and **(B)** corresponding IFN-γ and **(C)** IL-17A expression by these cells, **(D)** percentages of Lin⁻ ST2/IL-33R⁻NKp46⁻ ILC and **(E)** corresponding IFN-γ and **(F)** IL-17A expression. Error bars represent SEM and *p* values were calculated using One-way ANOVA followed by Tukey's multiple comparison test (black lines) and paired student's *t* test (grey lines). $^{*}p < 0.05$, $^{**}p < 0.01$, $^{***}p < 0.001$, $^{****}p < 0.0001$. Representative FACS plots show IFN-γ expression by Lin⁻ ST2/IL-33R⁻ NKp46⁺ (top) and NKp46⁻ (bottom) ILC. Experiments for each group was repeated minimum 2–3 times.

control showed elevated NKp46⁻ ILC1/ILC3 numbers, low or no expression of IFN-γ was observed **(**Fig. 2**D, E and S3)**. Remarkably, rMVAΔIL-1βR induced the highest IL-17A expression by both NKp46⁺ **(**Fig. 2**C)** and NKp46⁻ ILC1/ILC3 subsets **(**Fig. 2**F)**. rMVA and Influenza A vectors induced modest IL-17A expression by both these subsets, whilst rFPV, Ad5 and RV showed no IL-17A expression, similar to the unimmunized control **(**Fig. 2**C and F)**.

Unlike i.n., following i.m. delivery, the proportion of NKp46⁺ ILC1/ILC3 in the muscle was very minimal (0–0.8%) across all vaccine vectors **(**Fig. 2**A and** Fig. 3**A)**, with significant differences observed between rMVA compared to rFPV, rMVAΔIL-1βR and Ad5 ($p = 0.0087p = 0.0049$, and $p = 0.0397$ respectively). Additionally, only rFPV and Influenza A vaccinated groups showed any expression of IFN-γ by NKp46⁺ ILC1/ILC3 (Fig. 3**B)**. Interestingly, IFN-γ expression by these subsets was much greater following i.m versus i.n. vaccination (rFPV i.m. ∼12.06% i.n. 2.5% and influenza A i.m. ∼ 4.67% i.n. ∼1.5%) **(**Fig. 2**B and** Fig. 3**B)**. In the context of IL-17A expression by NKp46⁺ ILC1/ILC3, only Influenza A vaccinated animals showed any significant expression (average 8.39%, $p < 0.0001$ influenza A vs. all vaccine vectors) **(**Fig. 3**C)**. Of the poxviral vectors tested, rMVAΔIL-1βR vaccinated group also showed an increase in the proportion of NKp46⁺ ILC1/ILC3 expressing IL-17A (average 0.89%) although not significant and was similar to what was observed with i.n. delivery (average 1.0%).

Moreover, following i.m. delivery, different IFN-γ and IL-17A expression profiles were detected by NKp46⁻ ILC1/ILC3. Unlike i.n. delivery, very low IFN-γ expression was detected following i.m. vaccination, and only influenza A (∼0.01%) and Ad5 (∼0.03%) showed any IFN-γ expression **(**Fig. 2**E and** Fig. 3**E)**. All vectors showed different NKp46⁻ ILC1/ILC3-derived IL-17A expression profiles. Specifically, out of the vectors tested, Ad5 and rMVAΔIL-1βR showed the highest expression (∼0.58% and ∼0.84% respectively) **(**Fig. 3**F).** Interestingly, the NKp46⁻ ILC1/ILC3-derived IL-17A expression by the rMVAΔIL-1βR group was significantly elevated compared to unimmunised, rFPV, rMVA and influenza A ($p < 0.0001$, $p = 0.0064$, $p < 0.0001$, and $p < 0.0001$ respectively) **(Fig. S4)**. Whilst, Ad5 showed significant differences compared to unimmunised, rMVA, and influenza A vaccinated groups ($p = 0.0048$, $p = 0.0172$ and $p = 0.0219$ respectively) **(Fig. S4).**

2.3. rFPV and rMVAΔIL-1βR lead to preferential recruitment of CD11b⁺ CD103⁻ conventional DCs to the lung mucosae, 24 h post intranasal vaccination

Our previous studies have shown that transient inhibition of IL-13 at the vaccination site can significantly modulate DC recruitment and resulting avidity of CD8⁺ T cells, including B cell immunity [41,42,45]. Since we have shown that ILC2 are the major source of IL-13 at the vaccination site and this is also viral vector-dependent [44], in this study we have also assessed the influence of viral vector on lung DC recruitment 24 h post i.n. vaccination (as per indicated in **Figs. S5**). In this study, four different lung DC subsets was assessed (CD11b⁺ CD103⁻ cDC, CD11b⁻ CD103⁺ cross-presenting DC, CD11b⁻ CD8⁺ cross-presenting DC and CD11b⁻ B220⁺ pDC (not other immune cell infiltrates)). Percentage of each DC subset, for a given viral vector was calculated as a proportion of total MHC-II⁺ CD11c⁺ DCs, as described in Materials and Methods.

In agreement with Trivedi et al 2014, these studies also showed that rFPV recruited significantly elevated proportions of CD11b⁺

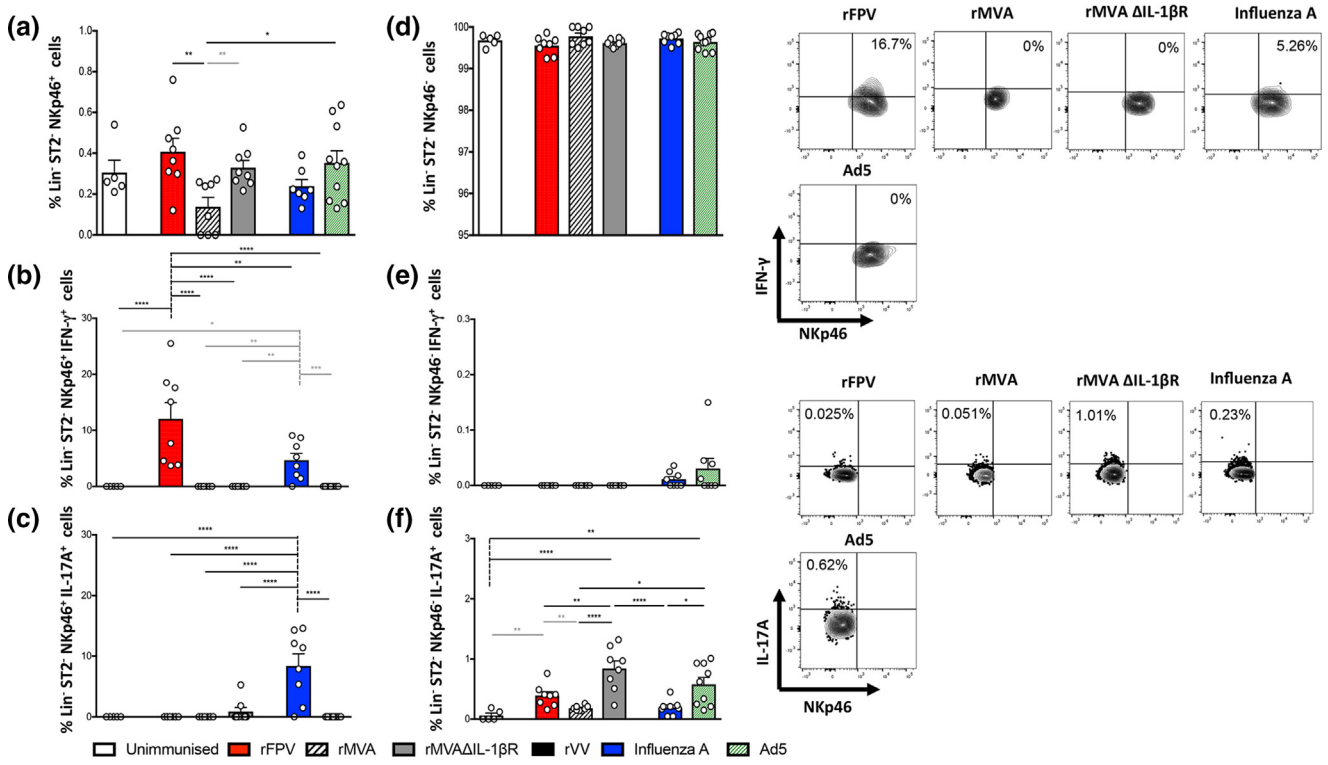

Fig. 3. Evaluation of muscle Lin$^-$ ST2$^-$ NKp46$^+$ and NKp46$^-$ ILC-derived IFN-γ and IL-17A profiles post intramuscular viral vector vaccination. BALB/c mice (n = 5–9) were i.m. immunised with rFPV, rMVA, rMVA-ΔIL-1βR, Influenza A or Ad5. 24 h post vaccination muscles were harvested and cell suspensions were stained for Lin$^-$ ST2/IL-33R$^-$ NKp46$^+$ and NKp46$^-$ ILC and their cytokine expression. Cells were pre-gated on CD45$^+$ FSC^{low} SSC^{low} cells as described in Materials and Methods and **Fig. S2**. **(A)** Graphs show percentage of Lin$^-$ ST2/IL-33R$^-$ NKp46$^+$ ILCs and **(B)** corresponding IFN-γ and **(C)** IL-17A expression by theses cells, **(D)** percentage of Lin$^-$ ST2$^-$ NKp46$^-$ ILCs and **(E)** their corresponding IFN-γ and **(F)** IL-17A expression. Error bars represent SEM and *p* values were calculated using One-way ANOVA followed by Tukey's multiple comparison test (black lines) and paired student's *t* test (grey lines). *$p < 0.05$, **$p < 0.01$, ***$p < 0.001$, ****$p < 0.0001$. Representative FACS plots show IFN-γ and IL-17A expression by Lin$^-$ ST2/IL-33R$^-$ NKp46$^+$ (top) and NKp46$^-$ (bottom) ILC. Experiments for each group was repeated minimum 2–3 times.

CD103$^-$ cDCs compared to rMVA and rVV ($p = 0.0062$, $p = 0.0322$ respectively). Additionally, the deletion mutant rMVAΔIL-1βR recruited the highest percentage of CD11b$^+$ CD103$^-$ cDCs, whilst Ad5 recruited the lowest (Fig. 4**A and B**). Furthermore, CD11b$^+$ CD103$^-$ cDC recruitment by Influenza A was similar to that of rFPV, rMVA, rVV and RV (Fig. 4**A and B**). Compared to the unimmunized control, rFPV, rMVAΔIL-1βR and Influenza A showed significant elevated CD11b$^+$ CD103$^-$ cDC recruitment ($p = 0.0069$, $p < 0.0001$ and $p = 0.0077$ respectively).

2.4. Intranasal rVV vaccination recruited elevated numbers of CD11b$^-$ CD103$^+$ and CD11b$^-$ CD8$^+$ cross-presenting DCs to the lung mucosae 24 h post vaccination

Unlike CD11b$^+$ CD103$^-$ cDC recruitment, rFPV induced significantly lower CD11b$^-$ CD103$^+$ cross-presenting DCs compared to that of the unimmunized control ($p = 0.0224$), and these values were significantly lower than that of rVV, Influenza A and RV vectors ($p < 0.0001$, $p = 0.0065$ and $p < 0.0001$ respectively) (Fig. 4**A and C**). Interestingly, compared to all viral vectors tested, rVV recruited the highest percentage of CD11b$^-$ CD103$^+$ cross-presenting DCs to the lung mucosae 24 h post vaccination. Whilst, rFPV recruited the lowest number similar to rMVA, rMVAΔIL-1βR and Ad5 (Fig. 4**C**). Furthermore, the proportion of CD11b$^-$ CD8$^+$ cross-presenting DCs recruited by all the vaccine vectors showed a comparable profile to that of the CD11b$^-$ CD103$^+$ cross-presenting DCs, where rVV showed the highest proportion of CD11b$^-$ CD8$^+$ cross-presenting DCs (Fig. 5**A and C**). It is noteworthy that the cross-presenting CD11b$^-$ CD103$^+$ DCs recruited by rVV, Influenza A and RV were significantly higher than unimmunized control ($p < 0.0001$, $p = 0.0067$ and $p = 0.0113$ respectively) (Fig. 4**A and C**). Whereas, cross-presenting CD11b$^-$ CD8$^+$ DCs recruited by rVV and Influenza A although were significantly higher than unimmunized control ($p < 0.0001$, $p = 0.0498$ respectively), Ad5 recruitment was significantly lower ($p = 0.0164$) (Fig. 5**A and C**).

2.5. Compared to the other viral vectors, RV and Ad5 recruited elevated CD11b$^-$ B220$^+$ plasmacytoid DCs to the lung mucosae 24 h post intranasal vaccination

Next when the CD11b$^-$ B220$^+$ pDC recruitment profile was assessed, these DCs showed a unique profile compared to the other three DC subsets examined. At 24 h post vaccination, RV and Ad5 recruited the highest percentage of CD11b$^-$ B220$^+$ pDCs to the lung mucosae, whilst Influenza A, rFPV and rMVAΔIL-1βR showed the lowest (Fig. 5**B and D**). Among the poxviral vectors, rVV recruited the highest proportion of CD11b$^-$ B220$^+$ pDCs whilst rFPV recruited the lowest, and rMVA and rMVAΔIL-1βR showed a similar pDC profile. Compared to the unimmunised control, rVV, RV and Ad5 vectors showed significant differences in pDC recruitment 24 h post vaccination ($p = 0.0025$, $p < 0.0001$ and $p < 0.0001$ respectively) (Fig. 5**B and D**).

2.6. Following intranasal vaccination different viral vectors showed different kinetic profiles 0 to 48 h post vaccination

Next, we also evaluated the DC recruitment kinetics 0 to 48 h post vaccination. Distinct DC kinetic profiles for each of the vectors were detected over time. rFPV showed significant regulation of

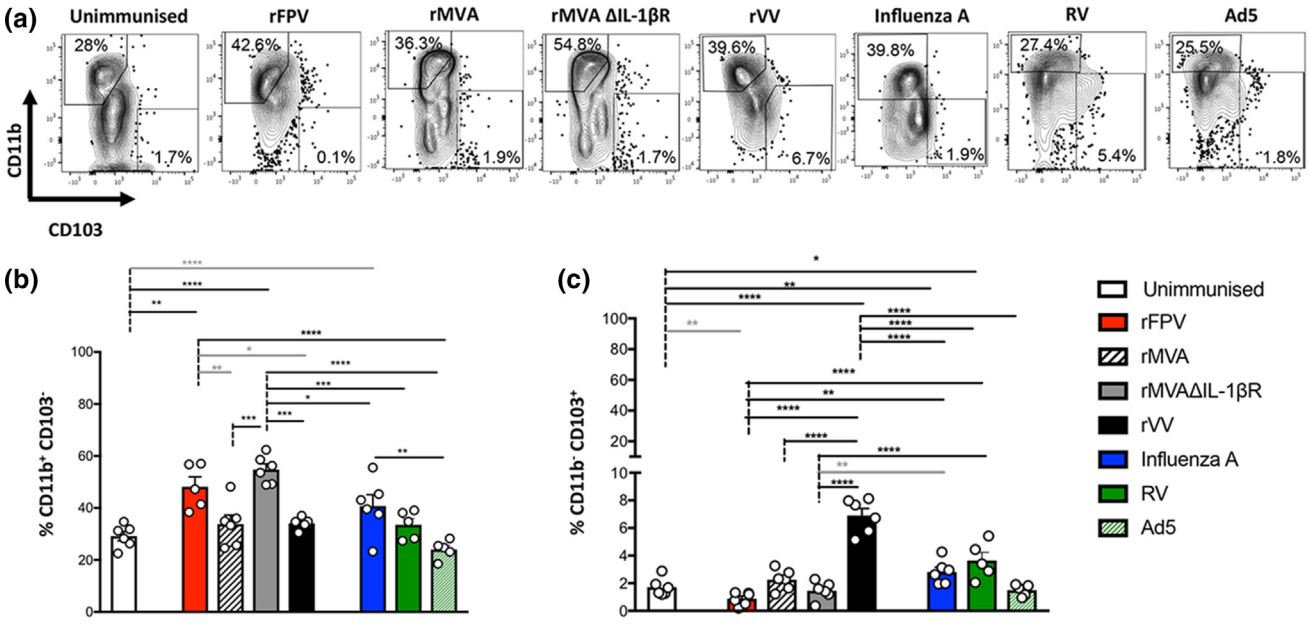

Fig. 4. Evaluation of CD11b$^+$ CD103$^-$ cDCs and CD11b$^-$ CD103$^+$ cross-presenting DCs following intranasal viral vector vaccination. BALB/c mice (n = 5) were i.n. immunised with rFPV, rMVA, rMVA-ΔIL-1βR, rVV, Influenza A, RV or Ad5. 24 h post vaccination lungs were harvested single cell suspensions were prepared and stained for different DC subsets and analysed using flow cytometry as described in Materials and Methods. Cells were pre-gated on MHC-II$^+$ CD11c$^+$ cells using fluorescence minus one (FMO) controls for each virus as described in Materials and Methods and **Fig. S5**. **(A)** Representative FACS plots show percentage of CD11b$^+$ CD103$^-$ DCs (gated top left) and CD11b$^+$ CD103$^-$ DCs (gated bottom right) recruited to lung mucosae. **(B)** Percentage of CD11b$^+$ CD103$^-$ DCs and **(C)** CD11b$^-$ CD103$^+$ DCs are shown as bar graphs, recruited by each vaccine vector. Percentages were calculated as a proportion of total MHC-II$^+$CD11c$^+$ DCs generated by each vector as indicated in Materials and Methods. Error bars represent SEM and p values were calculated using One-way ANOVA followed by Tukey's multiple comparison test (black lines) and paired student's t test (grey lines). $^*p < 0.05$, $^{**}p < 0.01$, $^{***}p < 0.001$, $^{****}p < 0.0001$. Experiments with each vector were repeated minimum 2–3 times.

CD11b$^+$ CD103$^-$ cDCs, which was similar to the cDC profile induced by the rMVA deletion variant (rMVAΔIL-1βR), unlike the parental rMVA (Fig. 6**A and S6**). The replication competent rVV showed regulation of all DC subsets, with significant modulation of cross-presenting DCs. Interestingly, cDC recruitment kinetics between rVV, rMVA and Influenza were very similar (Fig. 6**B and S6**). Ad5 recruited a pDC profile similar to RV and a CD11b$^-$ CD8$^+$ profile similar to rVV (Fig. 6**B, C and S6**).

3. Discussion

This study has clearly demonstrated that not only the route of vaccination, but also different viral vector-based vaccines can induce significantly different ILC subsets at the respective vaccination sites 24 h post delivery. In the context of ILC2, Lin$^-$ ST2/IL-33R$^+$ ILC2 were predominant in lung, whilst Lin$^-$ IL-25R$^+$ or/and Lin$^-$ TSLPR$^+$ ILC2 were found in muscle 24 h post viral vector vaccination. This was not entirely surprising as Lin$^-$ IL-25R$^+$ ILC2 has been associated with circulation [46,47], whilst Lin$^-$ TSLPR$^+$ ILC2 is known to be skin-resident [48]. Although, Lin$^-$ ST2/IL-33R$^+$ ILC2 was the major source of IL-13 in lung, Lin$^-$ IL-25R$^-$ TSLPR$^-$ ST2/IL-33R$^-$ ILC2s were the predominant source of IL-13 in muscle. Interestingly, recently we have also found that following viral vector vaccination IL-5 expression was specific to lung ILC2, not muscle (Jaeson *et al.* submitted), reaffirming that ILCs can be highly plastic under different conditions (specifically chronic inflammatory conditions versus vaccination or infection) [26,49], and why different routes of delivery may yield uniquely different innate and adaptive immune outcomes.

In addition to ILC2, i.n. versus i.m. vaccinations induced different proportions of NKp46$^+$ ILC1/ILC3s unlike NKp46$^-$ ILC1/ILC3s. Specifically, significantly lower numbers of NKp46$^+$ ILC1/ILC3s were detected in muscle compared to the lung (~1% vs 4–8%), confirming that circulatory ILC1/ILC3s are scarce as opposed to tissue resident ILCs [50]. Both NKp46$^+$ and NKp46$^-$ ILC1/ILC3s were able to express different levels of IFN-γ, that were vaccine route- and vector-dependent. Specifically, whilst both NKp46$^{+/-}$ ILC1/ILC3 subsets were able to express IFN-γ in lung, only the NKp46$^+$ ILCs in muscle expressed IFN-γ, albeit by two vaccination groups, where the expression was in the order of rFPV > Influenza A. Moreover, muscle NKp46$^-$cells expressed extremely low IFN-γ following Influenza and Ad5 vaccination. Majority of i.m. delivered vectors induced elevated ILC2-driven IL-13 and minimal ILC1/ILC3-driven IFN-γ expression compared to i.n. delivery. Additionally, our previous studies with pox-viral vectors have shown that, compared to i.m., i.n. delivery can induce T cells of higher avidity, associated with low IL-13 at the vaccination site [5,6,44]. Furthermore, i.n. rFPV priming has shown to induce high avidity T cells compared to i.n. rVV and Influenza priming vaccination [3,7,51], (Tan, Derose et al. personal communication). In agreement with our current study, i.n. Ad5 vaccination has also shown comparable ILC2 gene expression profiles to i.n. rFPV, unlike i.m. Ad5 delivery (Jaeson et al. submitted). Taken together, these findings may explain why systemic vaccination with some viral vectors may lead to suboptimal antiviral immunity, compared to mucosal vaccination [6,7,52,53].

Besides the route of delivery, each viral vector also induced a uniquely different ILC2-driven IL-13 and ILC1/ILC3-driven IFN-γ expression profiles. Specifically, both i.n. and i.m. rFPV vaccination induced low ILC2-derived IL-13, and high NKp46$^+$ or NKp46$^-$ ILC1/ILC3-derived IFN-γ. In contrast, i.m. rMVA vaccination induced lower ILC2-derived IL-13 compared to i.n. delivery. Knowing that, low IL-13 is associated with improved T cell immunity, our current data may explain why previously rMVA has been found to be more efficacious as an i.m. delivery vector than a mucosal delivery vector [8,10]. Moreover, whilst i.n. delivery of rMVA, Influenza A, RV and Ad5 induced elevated ILC2-derived IL-13, the expression of IFN-γ was lower in NKp46$^+$ ILC1/ILC3s following rMVA, Influenza A;

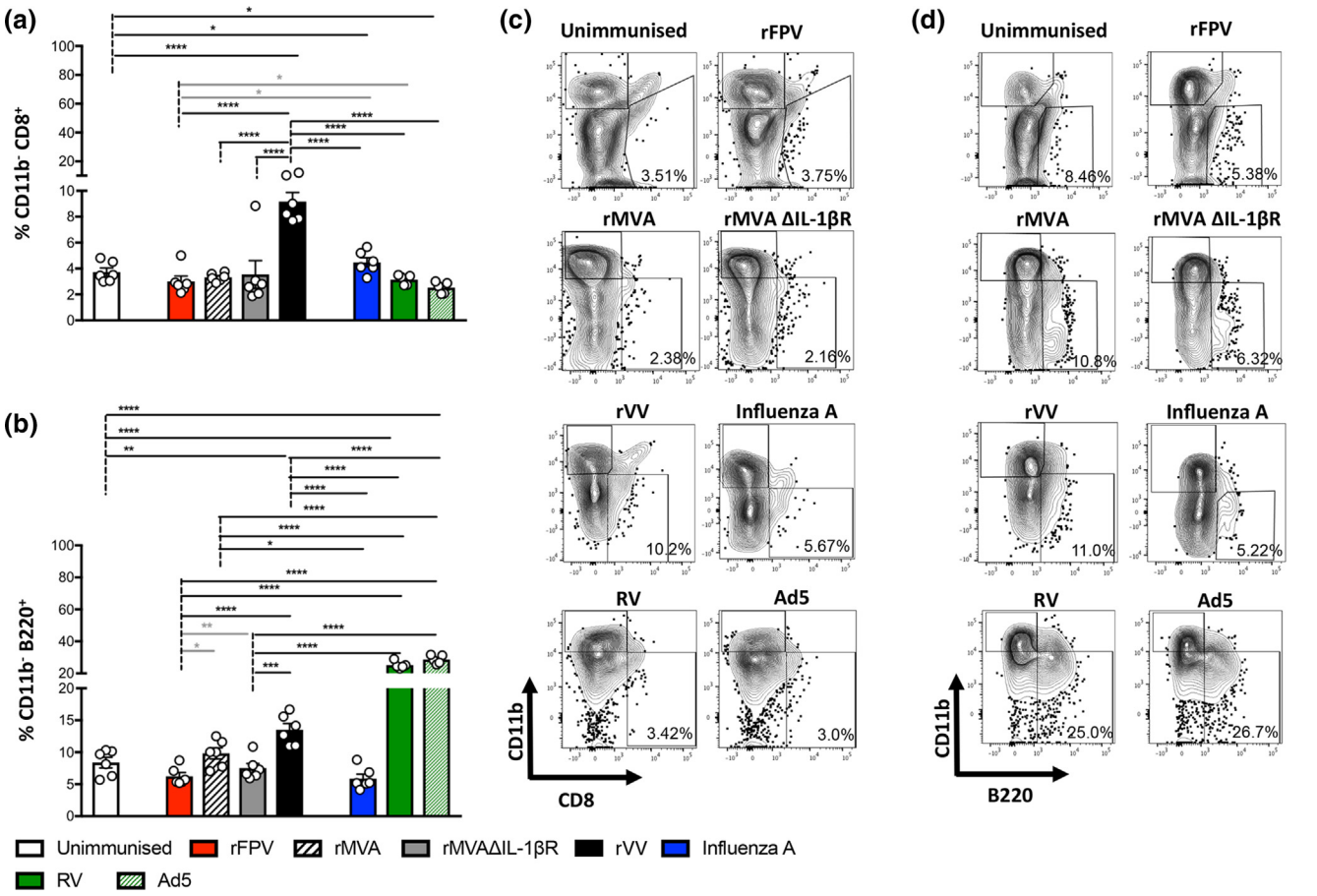

Fig. 5. Evaluation of CD11b$^-$ CD8$^+$ cross-presenting and CD11b$^-$ B220$^+$ pDC subsets following intranasal viral vector vaccination. BALB/c mice (n = 5) were i.n. immunised with same vectors as in Fig. 4 and lung cells were analysed using flow cytometry for DC subsets as per described in Materials and Methods. Cells were pre-gated on MHC-II$^+$ CD11c$^+$ cells using fluorescence minus one (FMO) controls as described in **Fig. S5**. Left panel bar graphs show **(A)** percentage of CD11b$^-$ CD8$^+$ DCs and **(B)** CD11b$^-$ B220$^+$ DCs recruited to the lung mucosae compared to the unimmunised control. Right panel representative FACS plots show percentage of **(C)** CD11b$^-$ CD8$^+$ DCs and **(D)** CD11b$^-$ B220$^+$ DCs recruited to the vaccination site 24 h post vaccination by each vector. Percentages were calculated as a proportion of total MHC-II$^+$CD11c$^+$ DCs generated by each vector as indicated in Materials and Methods. Error bars represent SEM and *p* values were calculated using One-way ANOVA followed by Tukey's multiple comparison test (black lines) and paired student's *t* test (grey lines). $^*p < 0.05$, $^{**}p < 0.01$, $^{***}p < 0.001$, $^{****}p < 0.0001$. Experiments with each vector were repeated minimum 2–3 times.

and NKp46$^-$ ILC1/ILC3s following RV and Ad5 vaccinations. Interestingly, we have previously shown that IL-4R antagonist adjuvanted vaccination that transiently inhibited IL-13 signalling via STAT6, induced low ILC2-derived IL-13 expression associated with elevated expression of NKp46$^-$ ILC1/ILC3-derived IFN-γ [44]. Additionally, enhanced *Ifngr* gene expression on ILC2 was also recently associated with low ILC2-derived IL-13 (Jaeson et al. submitted). Taken together, these observations suggest that enhanced ILC1/ILC3-derived IFN-γ expression regulates ILC2-derived IL-13 at the vaccination site, similar to the Th1/Th2 paradigm. Hence, we propose that ILC-derived IL-13 and IFN-γ balance at the vaccination site crucially impacts the downstream vaccine-specific immunity.

Different vectors also lead to differential expression of IL-17A by NKp46$^+$ and NKp46$^-$ ILC1/ILC3. Specifically, i.n. rMVA, rMVAΔIL-1βR and Influenza A vectors induced elevated IL-17A by both ILC1/ILC3 subsets at the lung mucosae 24 h post vaccination. However, majority of the vectors induced different levels of IL-17A by NKp46$^-$ ILC1/ILC3 subsets in the muscle. In asthma studies the importance of maintaining IL-13 and IL-17 balance has been well documented [54]. Similarly, our vaccination studies have also shown that IL-13 can regulate IL-17A expression on T cells at the transcriptional and translational level, and IL-17A is associated with T cell mediated protective immunity [55]. Knowing that (i) rVV and its derivatives (rMVA) perform better as a booster vaccine than a prime [7,8] (ii) Influenza A prime yield poor adaptive immune outcomes (Tan, Derose et al. personal communication) [51] and (iii) systemic Ad5 immunization have shown to induce less effective antiviral T cell responses [12,56–58], collectively our data suggest that the early onset of high ILC1/ILC3-derived IL-17A together with low IFN-γ and high ILC2-derived IL-13 could be detrimental for inducing effective cellular immunity.

Our study demonstrated that in addition to different ILC profiles, mucosal vaccination with different viral vectors yielded uniquely different lung DC profiles at the vaccination site 24 h post vaccination. We have previously shown that IL-13 levels at the vaccination site can significantly alter DC phenotype, specifically, inhibition of IL-13 can recruit elevated CD11b$^+$ CD103$^-$ cDCs associated with high avidity T cells [45]. This study further substantiated our previous findings of enhanced recruitment of CD11b$^+$ CD103$^-$ cDCs as opposed to CD11b$^-$ CD103$^+$ cross-presenting DCs following i.n. rFPV vaccination. Moreover, moderate proportions of CD11b$^-$ B220$^+$ pDCs were also observed with rFPV vaccination. pDCs are known to induce antibody differentiation via IFN-γ production [40] and their clustering with cDCs have shown to induce efficient T cell mediated antiviral immunity [38]. We have already established that rFPV priming can induce robust high avidity T cells and differentiated antibodies, involved in protective immunity against viral pathogens such as HIV [7,41]. Thus, our current findings suggest that although in the context of certain viral vectors, the cDC/pDC balance may govern the quality of T and

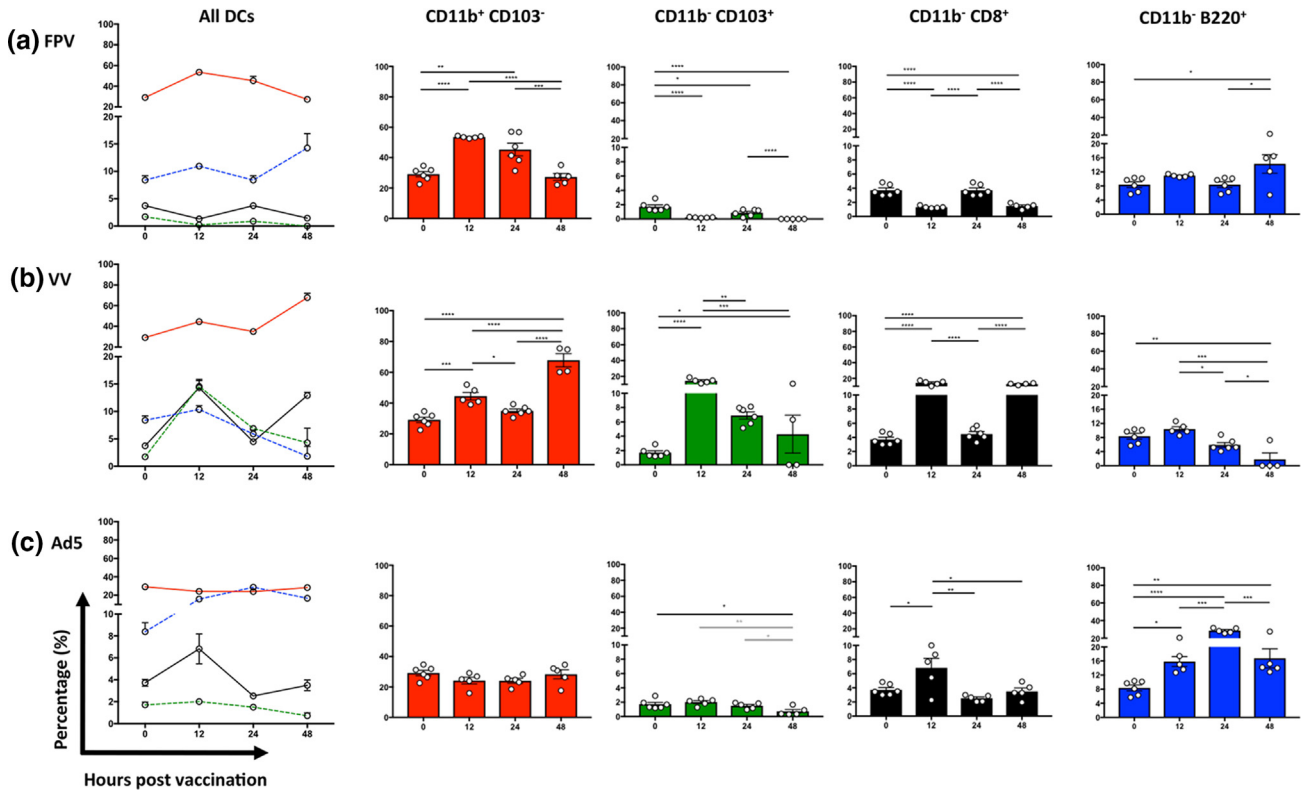

Fig. 6. DC kinetics following intranasal viral vector based vaccination 0–48 h post vaccination. BALB/c mice (n = 5) were i.n. immunised with rFPV, rVV and Ad5. Lungs were harvested at 12, 24 and 48 h post vaccination and lung DC subsets and analysed using flow cytometry as described in Materials and Methods. Cells were pre-dated on MHC-II$^+$ CD11c$^+$ cells using fluorescence minus one (FMO) controls as described in **Fig. S5.** Line graphs (left panel) and bar graphs (right four panels) show percentage of CD11b$^+$ CD103$^-$ DCs (red), CD11b$^-$ CD103$^+$ DCs (green), CD11b$^-$ CD8$^+$ DCs (black) and CD11b$^-$ B220$^+$ DCs (blue) recruited by **(A)** rFPV, **(B)** rVV and **(C)** Ad5 to the lung mucosae 0 to 48 h post vaccination. Error bars represent SEM and *p* values were calculated using One-way ANOVA followed by Tukey's multiple comparison test (black lines) and paired student's *t* test (grey lines). $^*p < 0.05$, $^{**}p < 0.01$, $^{***}p < 0.001$, $^{****}p < 0.0001$. Experiments with each vector were repeated minimum 2–3 times. (For interpretation of the references to colour in this figure legend, the reader is referred to the web version of this article.)

B cell immunity, replicating vectors such as Influenza A may employ other mechanisms (as Influenza A showed similar cDC/pDC profile to rFPV associated with poor quality T cells).

In contrast to rFPV vaccination, rMVA lead to elevated ILC2-derived IL-13, similar to rVV (data not shown), and both vectors significantly enhanced recruitment of CD11b$^-$ CD103$^+$ cross-presenting DCs to the lung mucosae, as shown previously [45]. This may explain why rMVA and rVV priming lead to low avidity T cells following recombinant HIV vaccination [3,7]. Moreover, intranasal Influenza A, RV and Ad5 vaccination which also lead to high ILC2-derived IL-13, preferentially induced CD11b$^-$ CD103$^+$ cross-presenting DCs as opposed to cDCs. In a prime-boost vaccine modality, recombinant Influenza A priming has shown to induce enhanced magnitude of vaccine-specific T cells, however, are of low avidity unlike rFPV priming (Tan, Derose et al. personal communication). Similarly, recombinant Ad5 vaccination has also shown to induce high magnitude of vaccine-specific CD8 T cells [13]. Therefore, these observations suggest that these vectors although lead to enhanced magnitude of vaccine-specific T cell immunity (IFN-γ production by T cells), may lead to low avidity T cells against chronic infections such as HIV-1. Despite low cDCs, Ad5 and RV exhibited a bias towards pDC recruitment. Knowing that pDC-driven IFN-γ can induce effective antibody responses, we postulate that Ad5- and RV-based vaccines could be more efficacious in inducing humoral immunity. Similar to CD11b$^-$ CD103$^+$ cross-presenting DCs, rVV additionally induced elevated CD11b$^-$ CD8$^+$ cross-presenting DCs to the lung mucosa. These observations suggested that, early induction of CD11b$^-$ CD8$^+$ cross-presenting DCs, could also be associated with induction of low avidity T cells. However, in the context of some pathogens, (for example, *Leishmania*, and also some viruses, Infleunza and HSV-1 infections), induction of cross-presenting DCs have been associated with protective immunity [30,59,60]. Thus, when designing recombinant viral vector-based vaccines, careful selection of the vector, according to the pathogen of interest may be of great importance.

rMVAΔIL-1βR is known to induce effective memory T cell responses compared to parental rMVA vaccination [61]. Unlike rMVA, rMVAΔIL-1βR induced low ILC2-derived IL-13 and elevated cDCs similar to rFPV, which has shown to induce high avidity T cells with better protective immunity. These findings indicated that removal of a single immune evasive gene from the viral vector can significantly alter the innate immune outcomes, specifically the ILCs and DCs, associated with effective protective immunity. However, compared to rFPV (which showed elevated IFN-γ and no IL-17A expression), rMVAΔIL-1βR vaccination induced suboptimal ILC1/ILC3-derived IFN-γ and high IL-17A expression at the vaccination site. It is well established that IFN-γ is crucial for antiviral immunity, and overexpression of IL-17A can lead to immune imbalance [62]. It is also known that viral IL-18 bp neutralize host IL-18 and prevent IFN-γ production [63]. Thus, the residual IL-18 bp in the rMVAΔIL-1βR vector could be responsible for the observed ILC1/ILC3-derived IFN-γ profile. Thus, we postulate that rMVA vector lacking both IL-1βR and IL-18 bp genes may lead to ILC/DC profiles similar to rFPV and balanced T and B cell outcomes.

Furthermore, rVV, rMVA and rMVAΔIL-1βR data clearly demonstrated that the attenuation status of a viral vector and the presence or absence of virokines significantly modulated the ILC cytokine expression and DC profile. The rFPV and rMVAΔIL-1βR

data indicated that viral vectors that do not interfere with the host immune system could be more efficacious at inducing vaccine-specific immunity in humans (e.g.- Avipoxvirus compared to Orthopoxvirus). These observations strongly highlight the notion that when designing viral vector-based vaccines, in addition to the safety and genetic stability, inherent properties of the viruses themselves need serious consideration (in this case, its replicative ability within the mammalian host).

We have previously shown that ILC2s are the only source of IL-13 at the vaccination site, 24 h post vaccination and IL-13 level in the milieu can crucially impact the DC recruitment at the lung mucosae [42,44,45]. Hence, collectively our findings suggest that, early ILC2-derived IL-13, together with ILC1/ILC3-derived IFN-γ and IL-17A, differentially impact DC recruitment/regulation at the vaccination site, associated with adaptive immune outcomes and this warrants further investigation. Therefore, we postulate that (i) following vaccination, ILC and DC profiles may act as predictors of downstream vaccine-specific immunity and (ii) selection of viral vector according to the pathogen of interest (eg: virus, bacteria or parasites) may help tailor/design effective viral-vector based vaccines against chronic pathogens.

4. Materials and Methods

Mice. Pathogen-free 6–8 weeks old female BALB/c mice were purchased from the Australian Phenomics Facility, The Australian National University. All animals were maintained, monitored daily and cervically dislocated at the endpoint according to the Australian NHMRC guidelines within the Australian Code of Practice for the Care and Use of Animals for Scientific Purposes and in accordance with guidelines approved by the ANU Animal Experimentation and Ethics Committee (AEEC), protocol number A2014/14 and A2017/15.

Viral vector-based Vaccines. Recombinant FPV, VV and MVA expressing HIV antigens described previously were used in this study [44,64]. The rMVAΔIL-1βR was constructed and kindly provided by Dr. Jackson. Influenza A and Adenovirus (Ad5) vectors were kindly provided by Prof. Arno Mullbacher, JCSMR, ANU. Recombinant Human Rhinovirus serotype 1A (RV) was kindly provided by Prof. Gowans and Dr. Wijesundara, Basil Hetzel Institute, University of Adelaide [16].

Immunisation. BALB/c mice were intranasally or intramuscularly immunised with $1x10^7$ plaque forming units (pfu) of each of the poxviruses rFPV, rVV, rMVA, rMVA-ΔIL-1βR; $2x10^7$ pfu (i.n.) or $2.5x10^7$ pfu (i.m.) of Ad5, 5×10^6 $TCID_{50}$ of RV or 500 pfu of Influenza A. Note that, doses used were comparable to those used in previous studies, optimal to induce adaptive immune outcomes. Mice were vaccinated with 10 μL per nostril (i.n.) or 50 μL per leg (i.m.) under mild isofluorane anaesthetic. rFPV, rVV, rMVA, rMVA-ΔIL-1βR were sonicated three times for 15 s on ice at 50% capacity using Branson Sonifier 450 immediately prior to vaccination.

Preparation of lung lymphocytes. Lung tissues were collected 24 h post vaccination in complete RPMI for ILC studies as described previously [44]. For DC studies, lungs were harvested at 12, 24 and 48 h post vaccination. Lung tissues were prepared as described previously [44]. Briefly, tissues were cut into small pieces, and enzymatically digested for 45 min at 37 °C in digestion buffer containing 1 mg/ml collagenase (Sigma-Aldrich, St Louis, MO), 1.2 mg/ml Dispase (Gibco, Auckland, NZ), 5 Units/ml DNase (Calbiochem, La Jolla, CA) in complete RPMI. Samples were crushed and passed through a 100 μm falcon cell strainer and resulting lung cell suspensions were then treated with red cell lysis buffer followed by extensive washing to remove the lysis buffer. Samples were then passed through gauze to remove debris, cells were re-suspended in complete RPMI, rested overnight at 37 °C under 5% CO_2 as per our previous studies prior to staining [5,42].

Preparation of muscle lymphocytes. Muscle tissues were harvested 24 h post vaccination in complete RPMI and prepared as previously indicated [44]. Briefly, tissues were, homogenised and enzymatically digested for 45 min at 37 °C in a digestion buffer containing 2 mg/mL collagenase, 2.4 mg/mL dispase and 5 Units/mL of DNAse in complete RPMI. Subsequently, samples were very gently pushed through a 70 μM Falcon cell strainer, to avoid debris. Resulting cell suspension was then washed, resuspended in complete RPMI and rested overnight as per lung prior to staining [5,42]

Evaluation of lung and muscle ILCs using flow cytometry. Monoclonal antibodies FITC-conjugated anti-mouse CD3 (T cells) clone 17A2, CD19 (B cells) clone 6D5, CD11b (macrophages and dendritic cells) clone M1/70, CD11c (dendritic cells) clone N418, CD49b (NK, NKT, T cells) clone HMα2, FcεRIα (Mast cells and Basophils) clone MAR-1 (all linage positive markers were selected as FITC), PE-conjugated anti-mouse ST2/IL-33R (clone DIH9), APC-conjugated IL-25R (clone 9B10), APC/Cy7-conjugated anti-mouse CD45 (clone 30-F11), Brilliant Violet 421-conjugated anti-mouse CD335 (NKp46) (clone 29A1.4), Brilliant Violet 510-conjugated anti-mouse IFN-γ (clone XMG1.2), Alexa Fluor 700-conjugated IL-17A (clone TC11-18H10.1) were obtained from BioLegend. PE-eFluor 610-conjugated anti-mouse IL-13 (clone eBio13A) was purchased from eBioscience and APC- conjugated anti-mouse TSLPR R&D systems. ILC2 and ILC1/3s were stained separately to avoid fluorochrome overlap. Specifically, FITC-conjugated lineage cocktail antibodies and APC/Cy7-conjugated anti-mouse CD45 were used in both ILC2 and ILC1/ILC3 staining. For lung and muscle ILC2 staining, PE-conjugated anti-mouse ST2/IL-33R, and PE-eFluor 610-conjugated anti-mouse IL-13 were used and for muscle ILC2 staining, additionally APC-conjugated IL-25R and APC-conjugated anti-mouse TSLPR were used. Brilliant Violet 421-conjugated anti-mouse NKp46, Brilliant Violet 510-conjugated anti-mouse IFN-γ, Alexa Fluor 700-conjugated IL-17A were only used in ILC1/3s staining. Briefly, for intracellular staining, samples were treated with Brefeldin A for 5 h, washed, cell surface staining was performed followed by and intracellular staining after fixing and permeabilising the cells as per our previous protocols[42]. Once the staining was completed all samples were fixed with 0.5% paraformaldehyde, 1.4×10^6 events from each lung sample were acquired and 3.0×10^6 events were acquired for muscle on a BD LSR Fortessa. Data were analysed using Tree Star FlowJo software (version 10.0.7) using gating strategies indicated in **Figs. S1 and S2**.

Evaluation of lung DCs using Flow cytometry. 2×10^6 cells were blocked with anti-mouse CD16/CD32 Fc Block antibody (BD Biosciences, USA) for 20 min at 4 °C and cells were surface stained with APC conjugated MHCII I-Ad (e-Biosciences, USA), biotin conjugated CD11c (N418 clone, Biolegend, USA), followed by streptavidin Brilliant violet 421 (Biolegend, USA) and other DC markers CD8 APC-eFluor780 (53–6.7 clone, ebiosciences, USA), B220 PercpCy5.5 (RA3-6B2 clone, e-Biosciences, USA), CD11b AlexaFluor 700 (M1170 clone, Biolegend, USA) and CD103 FITC (2E7 clone, e-Biosciences, USA) for 30 min on ice. Cells were resuspended in PBS and analysed using BD LSRII flow cytometer Becton Dickinson, San Diego, CA). 5×10^5 events per sample were collected and results were analyzed using FlowJo software version 10.0.7, as described in **Fig. S2**. Note that, live/dead staining was also performed using viability dye 7-amino-actinomycin D (7-AAD Biolegend, USA) **(Figs. S2A and S2B).**

Statistical analysis. Cytokine expression by ILCs was calculated as a percentage of the parent ILC subset**.** To depict the differences in IL-13 expression, following i.n. vs i.m. vaccinations, number of ILC2 expressing IL-13 were also back calculated to $CD45^+$ population and normalized to 1×10^6. The muscle ILC2 subset percent-

ages were calculated as (subset of interest/Lin$^-$ population $\times$ 100%). The DC subsets were represented as a percentage of total MHC-II$^+$ CD11c$^+$ DCs. The *p*-values were calculated using two-tailed paired parametric student's *t*-test, unpaired parametric student's *t*-test or Ordinary One-way ANOVA with Tukey's multiple comparison post-test. All experiments were repeated minimum 2–3 times.

5. Data availability

The authors declare that all data supporting the findings of this study are available within the paper and supplementary files.

Acknowledgements

The authors would like to thank Prof. Arno Mullbacher, JCSMR, ANU for the Influenza A and Adenovirus (Ad5) vectors; The Imaging and Cytometry facility for providing support with flow cytometry experiments; The Australian Phenomics Facility, ANU for maintenance and housing of mice used for the experiments. This work was supported by the Australian Centre for HIV and Hepatitis Virology Research (ACH2) grant, and National Health and Medical Research Council (NHMRC) Development grant APP1093532 and APP1136351 awarded to CR.

Author Contribution

SR designed and performed the DC studies, preparation of some vaccine stocks, analysis of the DC data and preparation of figures and the manuscript, SM performed most of the ILC studies and data analysis, ZL performed the RV and Ad5 ILC studies and data analysis, MIJ contributed to the ILC studies and manuscript preparation. RJJ constructed the rMVAΔIL-1βR. DKW, BG and EJG provided RV vaccine and critical evaluation of the manuscript. CR conceived the idea and helped design the experiments, data analysis and critical evaluation and preparation of the manuscript.

Disclosure

The authors declare no conflict of interest.

Appendix A. Supplementary material

Supplementary data to this article can be found online at https://doi.org/10.1016/j.vaccine.2019.01.045.

References

[1] Harari A, Bart PA, Stohr W, Tapia G, Garcia M, Medjitna-Rais E, et al. An HIV-1 clade C DNA prime, NYVAC boost vaccine regimen induces reliable, polyfunctional, and long-lasting T cell responses. J Exp Med 2008 Jan 21;205(1):63–77.
[2] Ibanga HB, Brookes RH, Hill PC, Owiafe PK, Fletcher HA, Lienhardt C, et al. Early clinical trials with a new tuberculosis vaccine, MVA85A, in tuberculosis-endemic countries: issues in study design. Lancet Infect Dis 2006 Aug;6(8):522–8.
[3] Ranasinghe C, Medveczky JC, Woltring D, Gao K, Thomson S, Coupar BE, et al. Evaluation of fowlpox-vaccinia virus prime-boost vaccine strategies for high-level mucosal and systemic immunity against HIV-1. Vaccine 2006 Jul 26;24(31–32):5881–95.
[4] Rerks-Ngarm S, Pitisuttithum P, Nitayaphan S, Kaewkungwal J, Chiu J, Paris R, et al. Vaccination with ALVAC and AIDSVAX to prevent HIV-1 infection in Thailand. N Engl J Med 2009;361(23):2209–20.
[5] Ranasinghe C, Eyers F, Stambas J, Boyle DB, Ramshaw IA, Ramsay AJ. A comparative analysis of HIV-specific mucosal/systemic T cell immunity and avidity following rDNA/rFPV and poxvirus-poxvirus prime boost immunisations. Vaccine 2011;29(16):3008–20.
[6] Ranasinghe C, Turner SJ, McArthur C, Sutherland DB, Kim JH, Doherty PC, et al. Mucosal HIV-1 pox virus prime-boost immunization induces high-avidity CD8+ T cells with regime-dependent cytokine/granzyme B profiles. J. Immunol. (Baltimore, Md : 1950) 2007;178(4):2370–9.
[7] Wijesundara DK, Ranasinghe C, Jackson RJ, Lidbury BA, Parish CR, Quah BJ. Use of an in vivo FTA assay to assess the magnitude, functional avidity and epitope variant cross-reactivity of T cell responses following HIV-1 recombinant poxvirus vaccination. PLoS ONE 2014;9(8):e105366.
[8] Gherardi MM, Najera JL, Perez-Jimenez E, Guerra S, Garcia-Sastre A, Esteban M. Prime-boost immunization schedules based on influenza virus and vaccinia virus vectors potentiate cellular immune responses against human immunodeficiency virus Env protein systemically and in the genitorectal draining lymph nodes. J Virol 2003;77(12):7048–57.
[9] Keefer MC, Frey SE, Elizaga M, Metch B, De Rosa SC, Barroso PF, et al. A phase I trial of preventive HIV vaccination with heterologous poxviral-vectors containing matching HIV-1 inserts in healthy HIV-uninfected subjects. Vaccine 2011;29(10):1948–58.
[10] Marthas ML, Van Rompay KK, Abbott Z, Earl P, Buonocore-Buzzelli L, Moss B, et al. Partial efficacy of a VSV-SIV/MVA-SIV vaccine regimen against oral SIV challenge in infant macaques. Vaccine 2011 Apr 12;29(17):3124–37.
[11] Barouch DH, O'Brien KL, Simmons NL, King SL, Abbink P, Maxfield LF, et al. Mosaic HIV-1 vaccines expand the breadth and depth of cellular immune responses in rhesus monkeys. Nat Med 2010;16(3):319–23.
[12] Buchbinder SP, Mehrotra DV, Duerr A, Fitzgerald DW, Mogg R, Li D, et al. Efficacy assessment of a cell-mediated immunity HIV-1 vaccine (the Step Study): a double-blind, randomised, placebo-controlled, test-of-concept trial. Lancet 2008;372(9653):1881–93.
[13] Shiver JW, Fu TM, Chen L, Casimiro DR, Davies ME, Evans RK, et al. Replication-incompetent adenoviral vaccine vector elicits effective anti-immunodeficiency-virus immunity. Nature 2002;415(6869):331–5.
[14] Hansen SG, Ford JC, Lewis MS, Ventura AB, Hughes CM, Coyne-Johnson L, et al. Profound early control of highly pathogenic SIV by an effector memory T-cell vaccine. Nature 2011;473(7348):523–7.
[15] Kim MC, Lee YN, Kim YJ, Choi HJ, Kim KH, Lee YJ, et al. Immunogenicity and efficacy of replication-competent recombinant influenza virus carrying multimeric M2 extracellular domains in a chimeric hemagglutinin conjugate. Antiviral Res 2017;148:43–52.
[16] Tomusange K, Yu W, Suhrbier A, Wijesundara D, Grubor-Bauk B, Gowans EJ. Engineering human rhinovirus serotype-A1 as a vaccine vector. Virus Res 2015;4(203):72–6.
[17] Tomusange K, Wijesundara D, Gummow J, Wesselingh S, Suhrbier A, Gowans EJ, et al. Mucosal vaccination with a live recombinant rhinovirus followed by intradermal DNA administration elicits potent and protective HIV-specific immune responses. Sci Rep 2016;6(36658):36658.
[18] Garber DA, O'Mara LA, Zhao J, Gangadhara S, An I, Feinberg MB. Expanding the repertoire of modified vaccinia ankara-based vaccine vectors via genetic complementation strategies. PLoS ONE 2009;4(5):e5445.
[19] Garcia-Arriaza J, Najera JL, Gomez CE, Sorzano CO, Esteban M. Immunogenic profiling in mice of a HIV/AIDS vaccine candidate (MVA-B) expressing four HIV-1 antigens and potentiation by specific gene deletions. PLoS ONE 2010 Aug 24;5(8):e12395.
[20] Roberts DM, Nanda A, Havenga MJ, Abbink P, Lynch DM, Ewald BA, et al. Hexon-chimaeric adenovirus serotype 5 vectors circumvent pre-existing anti-vector immunity. Nature 2006;441(7090):239–43.
[21] Artis D, Spits H. The biology of innate lymphoid cells. Nature 2015;517(7534):293–301.
[22] Neill DR, Wong SH, Bellosi A, Flynn RJ, Daly M, Langford TK, et al. Nuocytes represent a new innate effector leukocyte that mediates type-2 immunity. Nature 2010;464(7293):1367–70.
[23] Klose CSN, Flach M, Mohle L, Rogell L, Hoyler T, Ebert K, et al. Differentiation of type 1 ILCs from a common progenitor to all helper-like innate lymphoid cell lineages. Cell 2014;157(2):340–56.
[24] Gladiator A, Wangler N, Trautwein-Weidner K, LeibundGut-Landmann S. Cutting edge: IL-17-secreting innate lymphoid cells are essential for host defense against fungal infection. J Immunol (Baltimore, Md : 1950) 2013;190(2):521–5.
[25] Spencer SP, Wilhelm C, Yang Q, Hall JA, Bouladoux N, Boyd A, et al. Adaptation of innate lymphoid cells to a micronutrient deficiency promotes type 2 barrier immunity. Science (New York, NY) 2014 Jan 24;343(6169):432–7.
[26] Lim AI, Menegatti S, Bustamante J, Le Bourhis L, Allez M, Rogge L, et al. IL-12 drives functional plasticity of human group 2 innate lymphoid cells. J Exp Med 2016;213(4):569–83.
[27] Silver JS, Kearley J, Copenhaver AM, Sanden C, Mori M, Yu L, et al. Inflammatory triggers associated with exacerbations of COPD orchestrate plasticity of group 2 innate lymphoid cells in the lungs. Nat Immunol 2016 Jun;17(6):626–35.
[28] Braciale TJ, Hahn YS. Immunity to viruses. Immunol Rev 2013 Sep;255(1):5–12.
[29] Heath WR, Carbone FR. Dendritic cell subsets in primary and secondary T cell responses at body surfaces. Nat Immunol 2009 Dec;10(12):1237–44.
[30] Helft J, Manicassamy B, Guermonprez P, Hashimoto D, Silvin A, Agudo J, et al. Cross-presenting CD103+ dendritic cells are protected from influenza virus infection. J Clin Investig 2012 Nov;122(11):4037–47.
[31] Ho AW, Prabhu N, Betts RJ, Ge MQ, Dai X, Hutchinson PE, et al. Lung CD103+ dendritic cells efficiently transport influenza virus to the lymph node and load viral antigen onto MHC class I for presentation to CD8 T cells. J Immunol (Baltimore, Md : 1950) 2011;187(11):6011–21.

[32] Ingulli E, Funatake C, Jacovetty EL, Zanetti M. Cutting edge: antigen presentation to CD8 T cells after influenza A virus infection. Journal of immunology (Baltimore, Md : 1950) 2009;182(1):29–33.
[33] Waithman J, Zanker D, Xiao K, Oveissi S, Wylie B, Ng R, et al. Resident CD8(+) and migratory CD103(+) dendritic cells control CD8 T cell immunity during acute influenza infection. PLoS ONE 2013;8(6):e66136.
[34] Hildner K, Edelson BT, Purtha WE, Diamond M, Matsushita H, Kohyama M, et al. Batf3 deficiency reveals a critical role for CD8alpha+ dendritic cells in cytotoxic T cell immunity. Science (New York, NY) 2008;322(5904):1097–100.
[35] Lukens MV, Kruijsen D, Coenjaerts FE, Kimpen JL, van Bleek GM. Respiratory syncytial virus-induced activation and migration of respiratory dendritic cells and subsequent antigen presentation in the lung-draining lymph node. J Virol 2009;83(14):7235–43.
[36] GeurtsvanKessel CH, Willart MA, Bergen IM, van Rijt LS, Muskens F, Elewaut D, et al. Dendritic cells are crucial for maintenance of tertiary lymphoid structures in the lung of influenza virus-infected mice. J Exp Med 2009;206 (11):2339–49.
[37] GeurtsvanKessel CH, Willart MA, van Rijt LS, Muskens F, Kool M, Baas C, et al. Clearance of influenza virus from the lung depends on migratory langerin +CD11b- but not plasmacytoid dendritic cells. J Exp Med 2008;205 (7):1621–34.
[38] Yoneyama H, Matsuno K, Toda E, Nishiwaki T, Matsuo N, Nakano A, et al. Plasmacytoid DCs help lymph node DCs to induce anti-HSV CTLs. J Exp Med 2005;202(3):425–35.
[39] Belyakov IM, Kuznetsov VA, Kelsall B, Klinman D, Moniuszko M, Lemon M, et al. Impact of vaccine-induced mucosal high-avidity CD8+ CTLs in delay of AIDS viral dissemination from mucosa. Blood 2006 Apr 15;107(8):3258–64.
[40] Cerutti A, Qiao X, He B. Plasmacytoid dendritic cells and the regulation of immunoglobulin heavy chain class switching. Immunol Cell Biol 2005 Oct;83 (5):554–62.
[41] Jackson RJ, Worley M, Trivedi S, Ranasinghe C. Novel HIV IL-4R antagonist vaccine strategy can induce both high avidity CD8 T and B cell immunity with greater protective efficacy. Vaccine 2014 Sep 29;32(43):5703–14.
[42] Ranasinghe C, Trivedi S, Stambas J, Jackson RJ. Unique IL-13Ralpha2-based HIV-1 vaccine strategy to enhance mucosal immunity, CD8(+) T-cell avidity and protective immunity. Mucosal Immunol 2013 Nov;6(6):1068–80.
[43] Hamid MA, Jackson RJ, Roy S, Khanna M, Ranasinghe C. Unexpected involvement of IL-13 signalling via a STAT6 independent mechanism during murine IgG2a development following viral vaccination. Eur J Immunol 2018.
[44] Li Z, Jackson RJ, Ranasinghe C. Vaccination route can significantly alter the innate lymphoid cell subsets: a feedback between IL-13 and IFN-γ. npj Vaccines 2018.
[45] Trivedi S, Jackson RJ, Ranasinghe C. Different HIV pox viral vector-based vaccines and adjuvants can induce unique antigen presenting cells that modulate CD8 T cell avidity. Virology 2014;468–470:479–89.
[46] Huang Y, Guo L, Qiu J, Chen X, Hu-Li J, Siebenlist U, et al. IL-25-responsive, lineage-negative KLRG1(hi) cells are multipotential 'inflammatory' type 2 innate lymphoid cells. Nat Immunol 2015;16(2):161–9.
[47] Huang Y, Mao K, Chen X, Kawabe T, Li W, Zhu J, et al. Inflammatory ILC2: An IL-25-activated circulating ILC population with a protective role during helminthic infection. J Immunol 2017;198.
[48] Kim BS, Siracusa MC, Saenz SA, Noti M, Monticelli LA, Sonnenberg GF, et al. TSLP elicits IL-33-independent innate lymphoid cell responses to promote skin inflammation. Sci Transl Med 2013;5(170):170ra16.
[49] Bernink JH, Krabbendam L, Germar K, de Jong E, Gronke K, Kofoed-Nielsen M, et al. Interleukin-12 and -23 control plasticity of CD127(+) Group 1 and Group 3 innate lymphoid cells in the intestinal lamina propria. Immunity 2015 Jul 21;43(1):146–60.
[50] Gasteiger G, Fan X, Dikiy S, Lee SY, Rudensky AY. Tissue residency of innate lymphoid cells in lymphoid and nonlymphoid organs. Science (New York, NY) 2015;350(6263):981–5.
[51] Tan HX, Gilbertson BP, Jegaskanda S, Alcantara S, Amarasena T, Stambas J, et al. Recombinant influenza virus expressing HIV-1 p24 capsid protein induces mucosal HIV-specific CD8 T-cell responses. Vaccine 2016 Feb 24;34 (9):1172–9.
[52] Belyakov IM, Ahlers JD. Comment on "trafficking of antigen-specific CD8+ T lymphocytes to mucosal surfaces following intramuscular vaccination". Journal of immunology (Baltimore, Md : 1950 2009;182(4):1779. author reply -80.
[53] Belyakov IM, Isakov D, Zhu Q, Dzutsev A, Berzofsky JA. A novel functional CTL avidity/activity compartmentalization to the site of mucosal immunization contributes to protection of macaques against simian/human immunodeficiency viral depletion of mucosal CD4+ T cells. J Immunol (Baltimore, Md : 1950) 2007;178(11):7211–21.
[54] Newcomb DC, Boswell MG, Zhou W, Huckabee MM, Goleniewska K, Sevin CM, et al. TH17 cells express a functional IL-13 receptor and IL-13 attenuates IL-17A production. J Allergy Clin Immunol 2011 Apr;127(4). 1006–13 e1–4.
[55] Ravichandran J, Jackson RJ, Trivedi S, Ranasinghe C. IL-17A expression in HIV-specific CD8 T cells is regulated by IL-4/IL-13 following HIV-1 prime-boost immunization. J Interferon Cytokine Res 2015;35(3):176–85.
[56] Lee J, Hashimoto M, Im SJ, Araki K, Jin HT, Davis CW, et al. Adenovirus serotype 5 vaccination results in suboptimal CD4 T Helper 1 responses in mice. J Virol 2017;91(5):01132–1216.
[57] Provine NM, Larocca RA, Penaloza-MacMaster P, Borducchi EN, McNally A, Parenteau LR, et al. Longitudinal requirement for CD4+ T cell help for adenovirus vector-elicited CD8+ T cell responses. J Immunol (Baltimore, Md : 1950) 2014;192(11):5214–25.
[58] Yang TC, Millar J, Groves T, Zhou W, Grinshtein N, Parsons R, et al. On the role of CD4+ T cells in the CD8+ T-cell response elicited by recombinant adenovirus vaccines. Mol Therapy : J American Soc Gene Therapy 2007;15(5):997–1006.
[59] Ashok D, Schuster S, Ronet C, Rosa M, Mack V, Lavanchy C, et al. Cross-presenting dendritic cells are required for control of Leishmania major infection. Eur J Immunol 2014 May;44(5):1422–32.
[60] Jirmo AC, Nagel CH, Bohnen C, Sodeik B, Behrens GM. Contribution of direct and cross-presentation to CTL immunity against herpes simplex virus 1. J Immunol (Baltimore, Md : 1950) 2009;182(1):283–92.
[61] Staib C, Kisling S, Erfle V, Sutter G. Inactivation of the viral interleukin 1beta receptor improves CD8+ T-cell memory responses elicited upon immunization with modified vaccinia virus Ankara. J General Virol 2005 Jul;86(Pt 7):1997–2006.
[62] Erbel C, Akhavanpoor M, Okuyucu D, Wangler S, Dietz A, Zhao L, et al. IL-17A influences essential functions of the monocyte/macrophage lineage and is involved in advanced murine and human atherosclerosis. J Immunol (Baltimore, Md : 1950) 2014;193(9):4344–55.
[63] Novick D, Kim SH, Fantuzzi G, Reznikov LL, Dinarello CA, Rubinstein M. Interleukin-18 binding protein: a novel modulator of the Th1 cytokine response. Immunity 1999 Jan;10(1):127–36.
[64] Coupar BE, Purcell DF, Thomson SA, Ramshaw IA, Kent SJ, Boyle DB. Fowlpox virus vaccines for HIV and SHIV clinical and pre-clinical trials. Vaccine 2006 Feb 27;24(9):1378–88.